Systems & Control Transactions

Original Research Article
Peer Reviewed Conference Proceeding
ESCAPE 36 - European Symposium on Computer Aided Process Engineering
Sheffield, UK. 21-24 June 2026

PSE PRESS

A Method for Uniquely Determining Robust Operating Conditions in Simulated Moving Bed Chromatography

Kensuke Suzuki[ab]*, Tomoyuki Yajima[a], and Yoshiaki Kawajiri[ac]

[a] Nagoya University, Department of Materials Process Engineering, Nagoya, Japan
[b] The University of Tokyo, Department of Chemical System Engineering, Tokyo, Japan
[c] LUT University, School of Engineering Science, Mukkulankatu, Finland
* Corresponding Author: k-suzuki@pse.t.u-tokyo.ac.jp.

ABSTRACT

In this study, we propose a method to uniquely determine robust operating conditions for simulated moving bed (SMB) chromatography, an essential continuous liquid-phase separation technique in the pharmaceutical industry, in the form of explicit algebraic equations. The proposed method incorporates process robustness—defined as the probability of meeting the target purities under flow-rate uncertainty due to pump errors—without requiring computationally expensive dynamic simulations. In a computational demonstration, the method achieved a joint probability of 0.960 for simultaneously attaining 99.9% purity in both extract and raffinate products.

Keywords: Adsorption, Process Design, Process Operations, Optimization, Design Under Uncertainty

INTRODUCTION

Simulated moving bed (SMB) chromatography is a continuous liquid-phase separation technique widely used in the pharmaceutical and petrochemical industries. SMB is based on the concept of true moving bed (TMB) chromatography (Fig. 1a), in which continuous separation is achieved by countercurrent contact between a liquid phase and a solid adsorbent. In SMB, the countercurrent separation in TMB is mimicked by connecting multiple chromatographic columns in a semi-closed loop and periodically switching the inlet/outlet ports (Fig. 1b). These ports serve to supply the feed and desorbent and to withdraw the two product fractions, extract and raffinate. The port roles are switched simultaneously in the direction of the internal fluid flow at fixed time intervals, referred to as the step time.

This dynamic port switching adds substantial operational complexity to SMB; consequently, it is highly challenging to determine robust operating conditions—four zone flow rates and the step time—that simultaneously enhance productivity and guarantee high purity as required in pharmaceutical applications, under unavoidable uncertainties such as pump errors. Mazzotti et al. proposed the well-known triangle theory [1], which enables

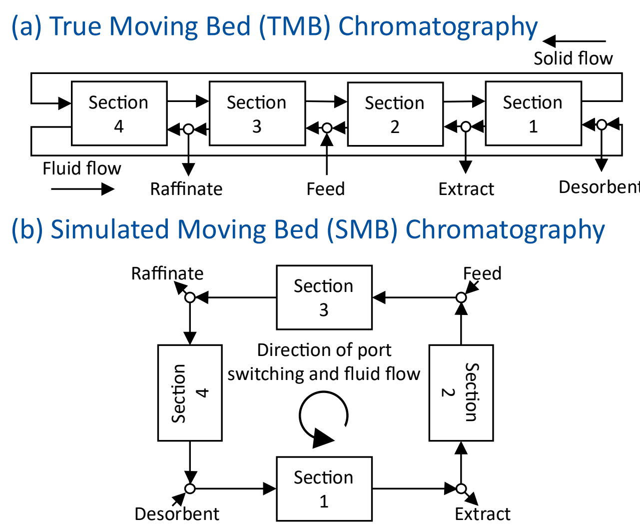

Figure 1. Schematic diagram of (a) true moving bed chromatography process and (b) simulated moving bed chromatography process.

SMB operating conditions to be determined solely from algebraic equations based on a TMB process model. Although Triangle Theory remains the most widely used method for selecting SMB operating conditions, it does not provide a systematic way to identify robust conditions in the presence of flow-rate uncertainties caused by pump errors. Note that they pointed out that the triangle theory can account for robust operation in a trial-and-error manner. Recently, sampling-based uncertainty quantification for SMB has been explored [2]; however, uncertainty quantification alone may require a large number of dynamic simulations, making the computational cost prohibitive for robust operating-condition determination.

In this study, we propose a method to uniquely determine robust SMB operating conditions under flow-rate uncertainty, without requiring any dynamic simulations. Specifically, the robust operating conditions under flow-rate uncertainty are derived analytically as explicit algebraic equations. This formulation enables a substantial reduction in computational cost for operating-condition selection. The robustness of the derived conditions is quantified by probability of achieving the target purities for the extract and raffinate products [3] and is validated computationally using dynamic simulations. In our case study, the probability that a purity of 99.9% is simultaneously achieved in both products was 0.960.

METHODS

Derivation of Unique Operating Condition

In this section, we present a method for uniquely determining robust SMB operating conditions in the presence of flow-rate uncertainty. Building on the triangle theory [1] as the theoretical foundation, we derive explicit algebraic equations for the robust operating conditions, expressed as dimensionless flow rates of the four zones (Fig. 1a, b), which are normalized by step time. According to the triangle theory, the dimensionless flow rate in jth zone, m_j, is defined as:

$$m_j = \left(Q_j t^{\mathrm{step}} - V_{\mathrm{zone}}\epsilon\right) / V_{\mathrm{zone}}(1-\epsilon),\ j = 1, 2, 3, 4, \quad (1)$$

where $Q_j, t^{\mathrm{step}}, V_{\mathrm{zone}}$, and ϵ are the volumetric flow rate in jth zone, step time, total zone volume, and the total porosity, respectively. In this study, the adsorption equilibrium of the two components is described by the following competitive Langmuir isotherm:

$$q_i^j = H_i C_i^j / \left(1 + b_1 C_1^j + b_2 C_2^j\right),\ i = 1, 2, \quad (2)$$

where q_i^j and C_i^j represent the solid-phase and the liquid-phase concentrations for ith component in jth zone, respectively; H_i and b_i refer to the Henry's constant and the affinity coefficient for ith component. Under Eq. (2), the triangle theory provides the conditions on m_j required to achieve complete separation—i.e., 100% purity for both extract and raffinate—through the following three inequalities:

$$H_2 < m_1 < \infty, \quad (3)$$

$$m_{2,\min}(m_2, m_3) < m_2 < m_3 < m_{3,\max}(m_2, m_3), \quad (4)$$

$$-\epsilon/(1-\epsilon) < m_4 < m_{4,\max}(m_2, m_3), \quad (5)$$

where $m_{2,\min}(\bullet), m_{3,\max}(\bullet)$, and $m_{4,\max}(\bullet)$ stand for algebraic functions defined by the triangle theory [1].

In this study, the uncertainty in the dimensionless flow rates of the four zones arising from pump errors is modeled by a four-dimensional multivariate normal distribution:

$$\widetilde{\boldsymbol{m}} \sim \mathrm{p}(\boldsymbol{m}) = N(\boldsymbol{m}, \boldsymbol{\Sigma}), \boldsymbol{m} = [m_1, m_2, m_3, m_4]^T \quad (6)$$

where $\widetilde{\boldsymbol{m}}$ denotes the uncertain (random) vector of dimensionless flow rates, and $\boldsymbol{m}$ is its mean vector. The matrix $\boldsymbol{\Sigma}$ is the covariance matrix; its entries $\Sigma_{k,l}$ are not necessarily zero. Derivation of $\boldsymbol{\Sigma}$ can be found in the literature [4].

The robust operating condition $\boldsymbol{m}^*$—i.e., the setpoint flow-rate vector to be specified for the pumps while accounting for pump errors—is determined by the following multiobjective optimization problem:

$$m_1^* = \arg\min_{\boldsymbol{m}} m_1 - H_2 \quad (7)$$

$$(m_2^*, m_3^*) = \arg\max_{\boldsymbol{m}} m_3 - m_2 \quad (8)$$

$$m_4^* = \arg\min_{\boldsymbol{m}} m_{4,\max}(m_2^*, m_3^*) - m_4 \quad (9)$$

s.t. all set of $\boldsymbol{m}$ in the following Eq. (10) satisfy Eqs. (3)-(5) simultaneously:

$$(\widetilde{\boldsymbol{m}} - \boldsymbol{m})^T \boldsymbol{\Sigma}^{-1} (\widetilde{\boldsymbol{m}} - \boldsymbol{m}) \leq \chi_{n=4}^2(\mu). \quad (10)$$

Here, the three objective functions in Eqs. (7)–(9) represent desorbent consumption, productivity, and enrichment, respectively. In Eq. (10), $\chi_{n=4}^2(\mu)$ is the μ-quantile of the chi-square distribution and n refers to the degrees of freedom. Because $\mu \in [0, 1)$, the conservativeness can be arbitrarily adjusted by controlling how much flow-rate uncertainty is considered. Note that this optimization problem cannot be solved analytically and therefore requires a numerical solution. In this study, we derive an analytical solution by reformulating it as a two-stage optimization [4]: Eq. (8) is treated as the primary objective function, while Eqs. (7) and (9) are considered as subsequent objectives.

Consequently, we derive a closed-form expression for the robust operating condition $\boldsymbol{m}^*$, given by the following explicit algebraic equations:

$$\begin{bmatrix} m_2^* \\ m_3^* \end{bmatrix} = -\boldsymbol{A}^{-1}\left(\boldsymbol{\Gamma}_{23} + \boldsymbol{n}_{23}\sqrt{\chi_{n=2}^2(\mu)}\right), \quad (11)$$

$$\begin{bmatrix} m_1^* \\ m_4^* \end{bmatrix} = \boldsymbol{\Gamma}_{14} + \boldsymbol{n}_{14}\sqrt{\chi_{n=2}^2(\mu)}, \quad (12)$$

$$\boldsymbol{A} = \begin{bmatrix} H_2 - H_1\left(1 + b_2 C_2^F\right) & b_2 C_2^F H_1 \\ H_2 - \omega_G\left(1 + b_2 C_2^F\right) & b_2 C_2^F \omega_G \end{bmatrix}, \quad (13)$$

$$\boldsymbol{\Gamma}_{23} = \begin{bmatrix} -H_1(H_2 - H_1) \\ -\omega_G(H_2 - \omega_G) \end{bmatrix}, \tag{14}$$

$$\boldsymbol{n}_{23} = \begin{bmatrix} \sqrt{[A_{11}, A_{12}] \begin{bmatrix} \Sigma_{22} & \Sigma_{23} \\ \Sigma_{32} & \Sigma_{33} \end{bmatrix} [A_{11}, A_{12}]^T} \\ \sqrt{[A_{21}, A_{22}] \begin{bmatrix} \Sigma_{22} & \Sigma_{23} \\ \Sigma_{32} & \Sigma_{33} \end{bmatrix} [A_{21}, A_{22}]^T} \end{bmatrix}, \tag{15}$$

$$\boldsymbol{\Gamma}_{14} = \begin{bmatrix} H_2 \\ m_{4,\max}(m_2^*, m_3^*) \end{bmatrix}, \tag{16}$$

$$\boldsymbol{n}_{14} = \begin{bmatrix} \sqrt{\Sigma_{11}} \\ \sqrt{\Sigma_{44}} \end{bmatrix}, \tag{17}$$

where C_i^F represents feed concentration for ith component and ω_G is a solution of quadratic equation given by the triangle theory [1]. Thus, without performing computationally expensive SMB dynamic simulations, the robust operating condition $\boldsymbol{m}^*$ can be determined simply by substituting the a priori identifiable parameters C_i^F, H_i, b_i, Σ, and μ into Eqs. (11) and (12).

Process Robustness Quantification

In this study, SMB process robustness is defined as the probability of achieving purities at or above the specified target purity, and this metric is used to evaluate the robust operating conditions $\boldsymbol{m}^*$ determined by Eqs. (11) and (12). This quantified process robustness is computed from the joint predictive distribution of the extract and raffinate purities, $\mathrm{p}(P_E, P_R)$, obtained under the flow-rate uncertainty $\mathrm{p}(\boldsymbol{m})$, as follows:

$$\mathrm{p}(P_E, P_R) = \int_{\mathcal{M}} \mathrm{p}(P_E, P_R|\boldsymbol{m})\mathrm{p}(\boldsymbol{m})d\boldsymbol{m} \tag{18}$$

where P_E and P_R refer to extract and raffinate purities, respectively; $\mathcal{M}$ denotes the uncertainty region defined by $\mathrm{p}(\boldsymbol{m})$; $\mathrm{p}(P_E, P_R|\boldsymbol{m})$ is a probabilistic model based on the SMB process model, which is formulated as a system of coupled partial differential–algebraic equations [3]. Additionally, the predictive distribution of the purity for a single product can be obtained by marginalizing the joint distribution $p(P_E, P_R)$, i.e., by integrating out the other purity variable, as follows:

$$\mathrm{p}(P_s) = \int_0^{100} \mathrm{p}(P_E, P_R)dp_{\hat{s}}\,, (s, \hat{s}) = (E, R), (R, E). \tag{19}$$

The process robustness is computed by integrating the joint predictive distribution $\mathrm{p}(P_E, P_R)$ from the specified target purities r_E and r_R up to 100 as follows:

$$\mathrm{P}(P_E \geq r_E, P_R \geq r_R) = \int_{r_E}^{100}\int_{r_R}^{100} \mathrm{p}(P_E, P_R)dP_E dP_R, \tag{20}$$

where $\mathrm{P}(P_E \geq r_E,\ P_R \geq r_R)$ is the joint probability that the purities of extract and raffinate simultaneously meet or exceed the target values r_E and r_R, respectively. Similarly to Eq. (19), the probability for a single product purity (i.e., the marginal probability) is obtained as follows:

$$\mathrm{P}(P_s \geq r_s) = \int_{r_s}^{100} \mathrm{p}(P_s)dP_s\,, s = R, E. \tag{21}$$

RESULTS

We determined the robust operating conditions $\boldsymbol{m}^*$ using Eqs. (11) and (12), and quantified the process robustness of $\boldsymbol{m}^*$ by the marginal probability (Eq. (21)) or the joint probability (Eq. (20)). The SMB scale and model parameters were taken from the study by Grosfils *et al.* [5], as shown in Table 1. Here, σ_{pump} denotes the standard deviation of the pump error used to construct the covariance matrix $\boldsymbol{\Sigma}$ in Eq. (6). Details of the derivation of $\boldsymbol{\Sigma}$ from σ_{pump} are available in the literature [4].

Table 1: Parameters used in this study [5].

parameter	value	parameter	value
C_1^F [g/L]	1.20	C_2^F [g/L]	1.20
H_1 [-]	3.23	H_2 [-]	6.50
b_1 [L/g]	0.210	b_2 [L/g]	0.422
ϵ [-]	0.620	V_{zone} [mL]	141
t^{step} [s]	300	σ_{pump} [mL/s]	0.124

When the conservativeness parameter μ is varied over $[0, 1)$, Eqs. (11) and (12) determine the four dimensionless flow rates $\boldsymbol{m}^*$ by reconciling the three objective functions in Eqs. (7)–(9), in particular at the expense of the primary objective, productivity (Eq. (8)). In this study, μ was set to six values: 0, 0.05, 0.25, 0.5, 0.75, and 0.99. Note that at $\mu = 0$, Eqs. (11) and (12) reduce exactly to the theoretical optimum in the triangle theory. As can be seen from Table 2, increasing μ leads to a simultaneous increase in m_1^*, m_2^*, and m_4^*, and a decrease in m_3^*; i.e. increasing μ results in higher desorbent consumption, lower productivity, and lower enrichment.

Table 2: Determined robust operating conditions $\boldsymbol{m}^*$ by the proposed method (Eqs. (11) and (12)). Note that $\boldsymbol{m}^*$ are shown to three decimal places for comparison across different μ values.

μ	m_1^*	m_2^*	m_3^*	m_4^*
0	6.500	2.491	3.968	2.556
0.05	6.547	2.609	3.970	2.555
0.25	6.611	2.771	3.972	2.556
0.50	6.672	2.925	3.974	2.560
0.75	6.744	3.105	3.977	2.570
0.99	6.944	3.609	3.984	2.644

For the target purities $r_E = r_R = 99.9$, the proposed method (Eqs. (11) and (12)) enabled the determination of robust operating conditions $\boldsymbol{m}^*$ with an arbitrary level of conservativeness by varying μ. Using dynamic simulations of the SMB process model [3], we estimated Eqs. (18) and (19) and quantified the process robustness of each of the six $\boldsymbol{m}^*$ in Table 2 using Eqs. (20) and (21). As shown in Table 3, $\mathrm{P}(P_E \geq r_E), \mathrm{P}(P_R \geq r_R)$, and $\mathrm{P}(P_E \geq r_E,\ P_R \geq$

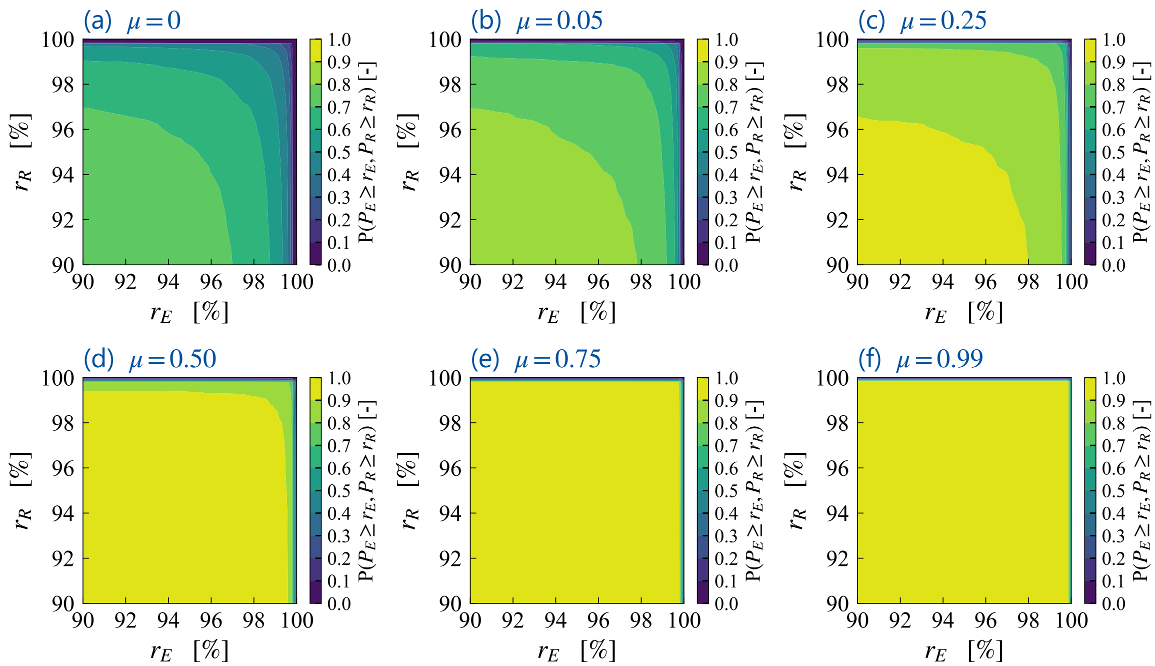

Figure 3: Comparison of six robust operating conditions by a contour plot of $P(P_E \geq r_E, P_R \geq r_R)$: (a) $\mu = 0$. (b) $\mu = 0.05$. (c) $\mu = 0.25$. (d) $\mu = 0.50$. (e) $\mu = 0.75$. (f) $\mu = 0.99$. The color bar on the right side of each contour plot refers to the value of $P(P_E \geq r_E, P_R \geq r_R)$.

r_R) all increase with μ. Particularly, at $\mu = 0.99$, all values exceed 0.950. Thus, $\mu = 0.99$ yields a robust operating condition $\boldsymbol{m}^*$ for $r_E = r_R = 99.9$.

Table 3: Values of process robustness at μ quantified by Eqs. (20) and (21) at the target purity as $r_E = r_R = 99.9$.

μ	$P(P_E \geq 99.9)$	$P(P_R \geq 99.9)$	$P\begin{pmatrix} P_R \geq 99.9, \\ P_E \geq 99.9 \end{pmatrix}$
0	0.113	0.133	0.0104
0.05	0.268	0.239	0.0646
0.25	0.485	0.436	0.245
0.50	0.651	0.617	0.462
0.75	0.802	0.789	0.689
0.99	0.973	0.978	0.960

When examining the response of the process robustness with the target purity treated as a variable, the trend of robustness of extract purity, $P(P_E \geq r_E)$, with respect to the target value r_E changes markedly depending on μ. As observed in Fig. 2a, increasing μ transforms $P(P_E \geq r_E)$ from a gently varying curve into a more sharply curved profile that remains close to $P(P_E \geq r_E) = 1.0$ over a wide range of r_E. This change in curvature indicates that the robustness of the extract purity is strongly influenced by μ.

In contrast, the robustness of the raffinate purity, $P(P_R \geq r_R)$, with respect to its target value r_R is less sensitive to μ than $P(P_E \geq r_E)$. As shown in Fig. 2b, even as μ is varied from 0 to 0.99, the overall profile remains similar: $P(P_R \geq r_R)$ decreases linearly for $r_R < 98.0$ and then exhibits a sharp drop at $r_R \approx 99.0$. The difference between the shapes of the $P(P_E \geq r_E)$and $P(P_R \geq r_R)$ curves in Figs. 2a and 2b arises from the shape of the shock fronts in the internal concentration profiles of the SMB process, as discussed in detail in the literature [3].

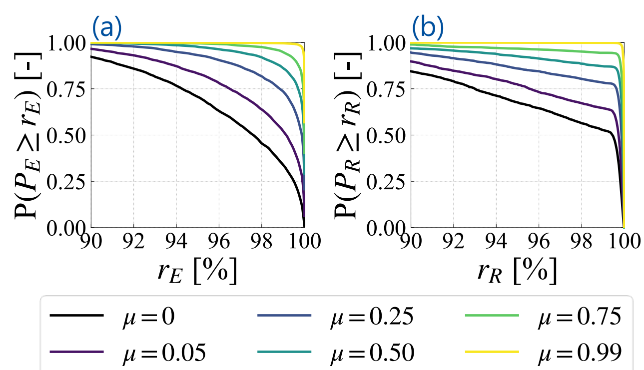

Figure 2. Comparison of process robustness with μ. (a) Change of robustness $P(P_E \geq r_E)$ through the target extract purity r_E. (b) Change of robustness $P(P_R \geq r_R)$ through the target raffinate purity r_R.

By comparing the joint probability $P(P_E \geq r_E, P_R \geq r_R)$ across the six μ values, we found that an appropriate choice of μ for efficient SMB operation under the flow-rate uncertainty depends on the target purities r_E and r_R. As shown in Fig. 3, an area where $\mathrm{P}(P_E \geq r_E,\, P_R \geq r_R) \geq 0.90$ first appear at $\mu = 0.25$ (Fig. 3c). With further increases in μ, the area expands; however, at $\mu = 0.75$ (Fig. 3e) most of the domain already attains $\mathrm{P}(P_E \geq r_E,\, P_R \geq r_R) \geq 0.90$, and little additional expansion is observed when increasing μ to 0.99 (Fig. 3f). Although, as shown in Table 2, the difference between $\mu = 0.75$ and $\mu = 0.99$ is pronounced for stringent targets of 99.9%, this difference becomes negligible for moderate targets such as 95.0 or 99.0. These results indicate that μ should be selected by simultaneously considering the desired process robustness at the specified target purities and the other performance metrics in Eqs. (7)–(9).

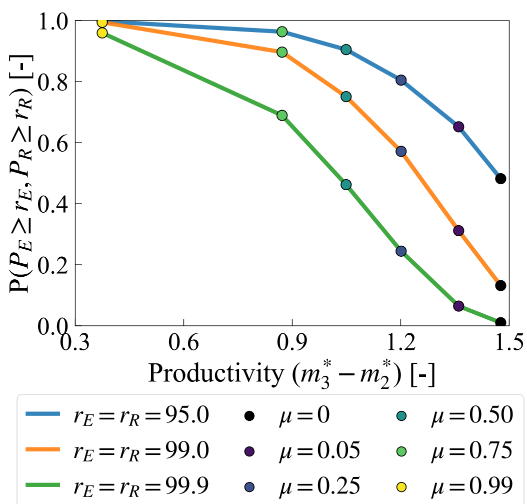

Figure 4. Trade-off relationship between productivity and robustness $\mathrm{P}(P_E \geq r_E, P_R \geq r_R)$ at three target purities.

The choice of an appropriate μ should be guided by the trade-off between process robustness (Eq. (20)) and productivity, which is treated as the primary objective function (Eq. (8)). As shown in Fig. 4, the trade-off curve for $r_E = r_R = 99.9$ is nearly linear, indicating that robustness can be increased at the expense of productivity in an approximately proportional manner. In contrast, the trade-off curves for targets of 95.0 and 99.0 are convex toward the upper right, implying diminishing returns: increasing μ beyond 0.75 yields little improvement in robustness. In particular, for the 95.0 target, the joint probability already satisfies $\mathrm{P}(P_E \geq 95.0,\, P_R \geq 95.0) \geq 0.90$ at $\mu = 0.50$. These results highlight that, within the proposed framework, selecting μ appropriately under the robustness–productivity trade-off is essential and should be tailored to the desired target purities.

CONCLUSION

We proposed a methodology to determine robust SMB operating conditions under flow-rate uncertainty in the form of explicit algebraic equations. We further evaluated the robustness and discussed an appropriate conservativeness parameter. Experimental validation of the method constitutes an important direction for future work.

ACKNOWLEDGEMENTS

This work was supported by the Japan Society for the Promotion of Science (JSPS) Grants-in-Aid for Scientific Research, Grant Number JP25K23521.

AUTHOR IDENTIFIERS

Author ORCIDs:
Kensuke Suzuki: 0000-0002-3628-5314
Tomoyuki Yajima: 0000-0002-7240-1693
Yoshiaki Kawajiri: 0000-0002-7124-1704

REFERENCES

1. Mazzotti M, Storti G, Morbidelli M. Optimal operation of simulated moving bed units for nonlinear chromatographic separations. Journal of Chromatography A 769:3-24 (1997). https://doi.org/10.1016/s0021-9673(97)00048-4
2. He Q, Zhao L. Bayesian inference based process design and uncertainty analysis of simulated moving bed chromatographic systems. Separation and Purification Technology 246:116856 (2020). https://doi.org/10.1016/j.seppur.2020.116856
3. Suzuki K, Yajima T, Kawajiri Y. Process robustness evaluation for various operating configurations of multi-column chromatography processes with nonlinear isotherm. Chemical Engineering Science 309:121395 (2025). https://doi.org/10.1016/j.ces.2025.121395
4. Suzuki K, Yajima T, Kawajiri Y. Quick robust design for simulated moving bed chromatography under comprehensive uncertainty via robust triangle theory. Separation and Purification Technology 391:136979 (2026). https://doi.org/10.1016/j.seppur.2026.136979
5. Grosfils V, Levrie C, Kinnaert M, Vande Wouwer A. A systematic approach to SMB processes model identification from batch experiments. Chemical Engineering Science 62:3894-3908 (2007). https://doi.org/10.1016/j.ces.2007.04.015